

2018

Uropathogenic enterobacteria use the yersiniabactin metallophore system to acquire nickel

Anne E. Robinson

Washington University School of Medicine in St. Louis

Jessica E. Lowe

Washington University School of Medicine in St. Louis

Eun-Ik Koh

Washington University School of Medicine in St. Louis

Jeffrey P. Henderson

Washington University School of Medicine in St. Louis

Follow this and additional works at: https://digitalcommons.wustl.edu/open_access_pubs

Recommended Citation

Robinson, Anne E.; Lowe, Jessica E.; Koh, Eun-Ik; and Henderson, Jeffrey P., "Uropathogenic enterobacteria use the yersiniabactin metallophore system to acquire nickel." *Journal of Biological Chemistry*. 293,39. . (2018).

https://digitalcommons.wustl.edu/open_access_pubs/8448

This Open Access Publication is brought to you for free and open access by Digital Commons@Becker. It has been accepted for inclusion in Open Access Publications by an authorized administrator of Digital Commons@Becker. For more information, please contact vanam@wustl.edu.

Uropathogenic enterobacteria use the yersiniabactin metallophore system to acquire nickel

Received for publication, June 14, 2018, and in revised form, August 10, 2018. Published, Papers in Press, August 14, 2018, DOI 10.1074/jbc.RA118.004483

Anne E. Robinson¹, Jessica E. Lowe, Eun-ik Koh, and Jeffrey P. Henderson²

From the Division of Infectious Diseases, Department of Internal Medicine, Department of Molecular Microbiology, Center for Women's Infectious Diseases Research, Washington University, St. Louis, Missouri, 63110

Edited by Ruma Banerjee

Invasive Gram-negative bacteria often express multiple virulence-associated metal ion chelators to combat host-mediated metal deficiencies. *Escherichia coli*, *Klebsiella*, and *Yersinia pestis* isolates encoding the *Yersinia* high pathogenicity island (HPI) secrete yersiniabactin (Ybt), a metallophore originally shown to chelate iron ions during infection. However, our recent demonstration that Ybt also scavenges copper ions during infection led us to question whether it might be capable of retrieving other metals as well. Here, we find that uropathogenic *E. coli* also use Ybt to bind extracellular nickel ions. Using quantitative MS, we show that the canonical metal–Ybt import pathway internalizes the resulting Ni–Ybt complexes, extracts the nickel, and releases metal-free Ybt back to the extracellular space. We find that *E. coli* and *Klebsiella* direct the nickel liberated from this pathway to intracellular nickel enzymes. Thus, Ybt may provide access to nickel that is inaccessible to the conserved NikABCDE permease system. Nickel should be considered alongside iron and copper as a plausible substrate for Ybt-mediated metal import by enterobacteria during human infections.

Escherichia coli and related enterobacteria are the predominant cause of human urinary tract infections (UTIs)³ and contribute substantially to the worldwide rise in antibiotic-resistant infections (1). Clinical enterobacterial isolates often possess additional, nonessential, virulence-associated genes. Prominent among these is the *Yersinia* high pathogenicity island (HPI), which encodes the biosynthetic machinery to make the specialized metabolites yersiniabactin (Ybt) and escherichelin (2). Direct mass spectrometric detection of urinary Ybt in UTI

patients, serological markers, transcriptional signatures, and experimental infection models all indicate active expression of *Yersinia* HPI proteins during UTI pathogenesis (3–7).

Although initially understood as a siderophore (a chelator that binds Fe(III) for bacterial use), Ybt has recently been appreciated to exhibit a broader metal ion–binding repertoire. Copper–Ybt complexes were observed in *E. coli* UTI patients and were connected to protection of *E. coli* from copper toxicity (7), an example of biological metal passivation. Because copper is an important nutrient, complete sequestration of copper ions by Ybt could starve uropathogenic *E. coli* (UPEC) of copper. However, UPEC retain nutritional access to Ybt-bound copper and iron by importing the metal–Ybt complexes in a controlled manner, extracting the metal, and using it to support metal-dependent cellular functions (8). These findings implicate Ybt as an agent of nutritional passivation, a biological strategy in which metal ion toxicity is minimized and nutritional access is preserved. In this manner, Ybt acts as an extracellular metal ion sink, with subsequent entry into the cell occurring as a controlled process. Whether this nutritional passivation activity of Ybt extends to biological metal ions beyond copper has been unclear.

Nickel is a trace element in human hosts whose unique redox chemistry is used by a series of microbial enzymes. *E. coli* acquire nutritional nickel ions via the conserved NikABCDE permease. Transcriptional up-regulation of this system during UTI (9) is indicative of nickel deficiency during infection (10–12). This is consistent with nickel scarcity in human hosts, where urinary nickel content (~0.04 μmol per liter) is lower than that of iron (~0.1 μmol per liter) (13, 14). Moreover, this trace nickel is thought to be predominantly bound by host-derived ligands (15, 16). Indeed, the NikA substrate is not free nickel Ni(II) but rather a Ni-(L-histidine)₂ complex (17). The ability of Ybt, another nitrogen heterocycle, to form nickel complexes raises the question of whether Ybt facilitates nutritional nickel uptake in uropathogenic *E. coli*. Indeed, K12 *E. coli* ectopically expressing the outer membrane *Yersinia* HPI–encoded ferric yersiniabactin uptake transporter (FyuA) import Ni–Ybt (18).

Yersinia HPI proteins involved in metal–Ybt uptake are encoded within two operons. These include the outer and inner membrane transport-associated proteins, FyuA and YbtPQ, respectively. The two other HPI operons encode Ybt biosynthesis-associated proteins and the transcription factor YbtA, which is necessary for expression of all four HPI operons (19).

This work was supported by NIDDK, National Institutes of Health Grants R01DK099534 and R01DK111930 (to J. P. H.). The authors declare that they have no conflicts of interest with the contents of this article. The funders had no role in study design, data collection and interpretation, or in the decision to submit the work for publication. The content is solely the responsibility of the authors and does not necessarily represent the official views of the National Institutes of Health.

This article contains supporting Fig. S1 and Table S1.

¹ Supported by the Mr. and Mrs. Spencer T. Olin Fellowship for Women in Graduate Study.

² To whom correspondence should be addressed: Box 8051, Washington University School of Medicine, 660 S. Euclid Ave., St. Louis, MO 63110. Tel.: 314-362-7250; Fax: 314-362-3203; E-mail: hendersonj@wustl.edu.

³ The abbreviations used are: UTI, urinary tract infection; HPI, high pathogenicity island; Ybt, yersiniabactin; UPEC, uropathogenic *E. coli*; Ni–Ybt, nickel–yersiniabactin; ICP-MS, inductively coupled plasma MS; rcf, relative centrifugal force; LC-MS/MS, LC-tandem MS.

Ybt-mediated nickel acquisition

FyuA is a β -barrel outer membrane protein which imports Ybt complexes into the periplasm using energy from the proton gradient across the inner membrane by coupling to the inner membrane TonB/ExbB/ExbD complex (20). YbtP and YbtQ are putative ABC transporters that are thought to form a heterodimer (termed YbtPQ) in the inner membrane and are necessary for cellular utilization of Ybt-bound iron (8, 18, 21). The precise YbtPQ-dependent mechanism through which metal–Ybt complexes are dissociated remains unclear although a reductive dissociation mechanism consistent with the observed, nondestructive extracellular release of metal-free Ybt has been proposed (8).

Connections between nickel-dependent enzymes and uropathogenesis suggest that *Yersinia* HPI-mediated nickel uptake could contribute to enterobacterial virulence during UTI. Although our knowledge of metal-dependent proteins in bacteria is incomplete (22), nickel is a critical part of the catalytic center for at least two *E. coli* nickel-dependent enzymes identified to date (23). [NiFe]-hydrogenases catalyze both H_2 oxidation and reduction during energy metabolism. Deletion of the [NiFe]-hydrogenase-containing formate hydrogenlyase complex, which is involved in mixed-acid fermentation of glucose (24), resulted in decreased UPEC fitness in a murine UTI model (9). Nickel-dependent urease catalyzes the hydrolysis of urea to ammonia and carbon dioxide and is common in *Klebsiella* and *Proteus*, where it is recognized as a classic urovirulence factor (25).

In this study we examined whether uropathogenic enterobacteria use the *Yersinia* HPI to interact with nickel. To assess passivation we used mutants to monitor the effect of Ybt synthesis on *E. coli* growth in nickel-toxic conditions. To interrogate the nutritional value of Ni–Ybt, we first used quantitative mass spectrometric approaches to monitor Ni–Ybt uptake and fate in defined uropathogenic *E. coli* mutants. We next determined whether Ni–Ybt import affects nickel-dependent enzyme activities in different uropathogen species. Our findings expand the substrates of nutritional passivation by the Ybt metallophore system of uropathogenic enterobacteria to include nickel.

Results

E. coli form nickel–yersiniabactin during growth in the presence of nickel ions

To determine whether uropathogenic *E. coli* form Ni–Ybt (18) during growth in culture, we grew the model uropathogenic *E. coli* strain UTI89 (26) in a minimal medium at a range of $NiCl_2$ concentrations (Fig. 1). We assessed yersiniabactin production and speciation in the conditioned media using an LC-tandem MS (LC-MS/MS) assay sensitive to Ybt and its different metal–Ybt complexes (7). Ni–Ybt, evident by its ~70:30 distribution of stable ^{58}Ni and ^{60}Ni isotopes (m/z 538, 540), characteristic precursor/product ion transition (m/z 538:351), and relative retention time (18), appeared in nickel-supplemented media. With increasing nickel concentrations, the population of the Ybt species shifted from predominantly metal-free Ybt (with 0 μM added $NiCl_2$) to predominantly Ni–Ybt (with $\geq 4 \mu M$ added $NiCl_2$) (Fig. 1a). These data demonstrate

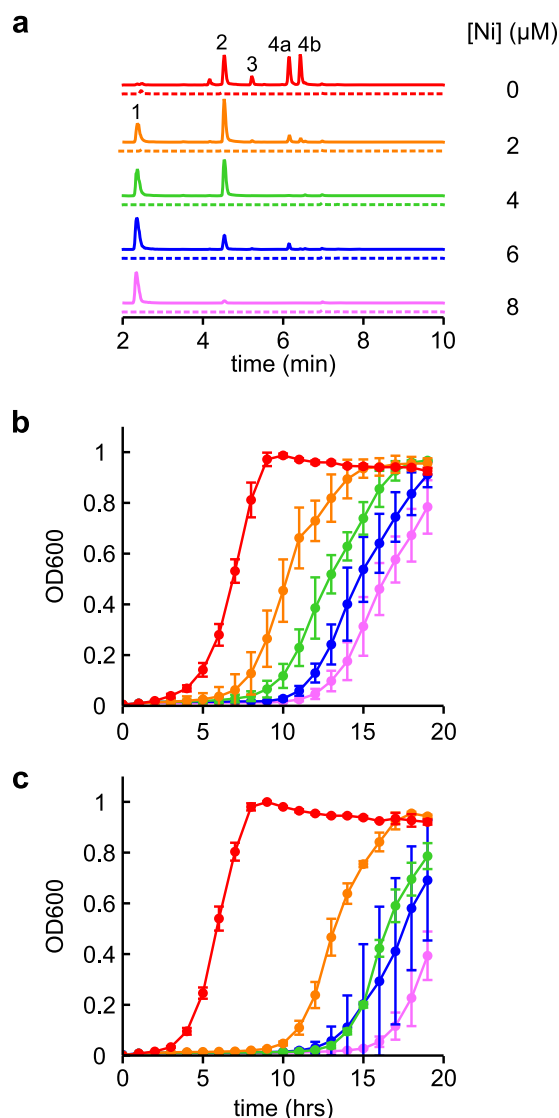


Figure 1. Ybt binds nickel ions and protects *E. coli* from nickel toxicity. a, representative LC-MS/MS (constant neutral loss) detecting Ybt species in the conditioned media of WT (solid lines) and $\Delta ybtS$ (dotted lines) UTI89 cultures grown in glucose minimal media at a range of $NiCl_2$ concentrations. As nickel concentrations increased, the levels of metal-free Ybt (4a and 4b) decreased concomitant with an increase of Ni–Ybt (1). The other observable peaks are Cu–Ybt (2) and Fe–Ybt (3). Ion chromatograms are presented with identical scaling. b and c, growth curves of WT (b) and $\Delta ybtS$ (c) UTI89 at the same range of $NiCl_2$ concentrations (indicated by color) were measured in the glucose minimal media. Growth curves were performed in triplicate, and results are shown as mean \pm S.D.

Ybt production and Ni–Ybt complex formation by uropathogenic *E. coli* in the presence of nickel.

Yersiniabactin protects *E. coli* from nickel toxicity

Macomber *et al.* (27) observed nickel toxicity in *E. coli* based upon inhibition of the glycolysis pathway. We observed a similar nickel-dependent lag in UTI89 growth while monitoring Ni–Ybt formation in a glucose-based medium (Fig. 1b). To determine whether Ybt counteracts growth inhibition by nickel, we compared growth of UTI89 to its isogenic, Ybt-deficient deletion mutant UTI89 $\Delta ybtS$ in the nickel-supplemented culture conditions described above. YbtS is a salicylate synthase encoded on the *Yersinia* HPI that is necessary

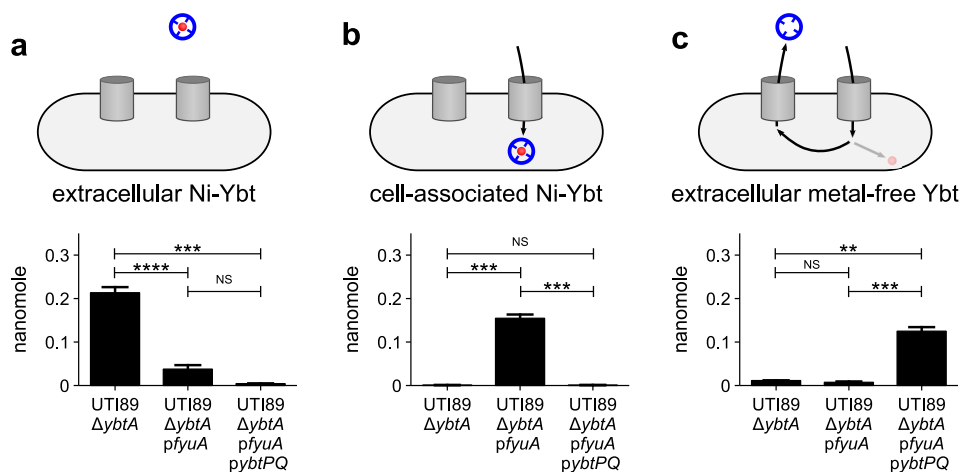


Figure 2. Uropathogenic *E. coli* import Ni-Ybt. *a–c*, UTI89 $\Delta ybtA$ expressing none, one, or both of the Ybt uptake components (*pfyA* and *pybtPQ*) were grown in M63 minimal media and exposed to 0.2 μM exogenous Ni-Ybt for 2 h prior to isolation and extraction of Ni-Ybt and metal-free Ybt from the supernatant (*a* and *c*, respectively) or cells (*b*). Ybt or Ni-Ybt were quantified by LC-MS/MS. Cartoons indicate which Ybt species was assessed in which graph. Experiments were performed in triplicate; results are shown as mean \pm S.D. **, $p \leq 0.01$; ***, $p \leq 0.001$; ****, $p \leq 0.0001$ based on a *t* test (two-tailed); NS, nonsignificant.

for Ybt production in minimal media (28). No detectable Ybt or metal-Ybt complexes were observed in LC-MS/MS profiles of UTI89 $\Delta ybtS$ -conditioned media (Fig. 1*a*). UTI89 $\Delta ybtS$ was more sensitive to growth inhibition by nickel than WT UTI89, exhibiting a more pronounced growth lag (Fig. 1*c*) similar to that observed by Macomber *et al.* (27). Ni-Ybt formation is thus associated with protection from nickel toxicity in UTI89. Together, these observations are consistent with Ybt-mediated nickel passivation by uropathogenic *E. coli*.

Uropathogens expressing the *Yersinia* HPI import Ni-Ybt and recycle metal-free Ybt

Although uropathogenic *E. coli* may encounter nickel toxicity in some environmental niches, nickel scarcity appears to be typical of host environments during urinary pathogenesis (9). Thus, if Ybt acted solely as an extracellular nickel ion sink, it would risk starving the cells for nutritionally important nickel ions. We therefore hypothesized that, as with copper, the Ybt system also facilitated controlled cellular delivery of nickel ions. To determine whether uropathogenic enterobacteria access Ybt-bound nickel, we used LC-MS/MS to monitor trafficking in an *E. coli* strain ectopically expressing the Ybt outer membrane receptor FyuA and the putative inner membrane heterodimeric transporter, YbtPQ. These transporters were expressed in UTI89 $\Delta ybtA$, a strain in which the *Yersinia* HPI is transcriptionally inactivated (8, 19, 29). We exogenously supplied purified Ni-Ybt (0.2 μM) to the culture medium and monitored its fate using quantitative LC-MS/MS (Fig. 2). In UTI89 $\Delta ybtA$ cultures, Ni-Ybt remained in the supernatant. FyuA expression (UTI89 $\Delta ybtA$ *pfyA*) caused Ni-Ybt depletion from the medium and accumulation in the cell-associated fraction, consistent with Ni-Ybt import to the periplasm (18). FyuA and YbtPQ coexpression (UTI89 $\Delta ybtA$ *pfyA pybtPQ*) caused Ni-Ybt depletion from both the medium and the cell-associated fraction and resulted in accumulation of metal-free Ybt in the medium. This pattern of FyuA-dependent uptake and YbtPQ-dependent Ybt recycling was observed previously for Fe-Ybt and Cu-Ybt (8, 18). Together, these findings are

consistent with a pathway of Ni-Ybt import, nickel extraction, and Ybt recycling in uropathogenic *E. coli* that express the canonical metal-Ybt import pathway.

UTI89 retain Ni-Ybt-derived nickel

We hypothesized that bacteria retain the nickel released following FyuA- and YbtPQ-dependent Ni-Ybt import and dissociation. To distinguish the nickel ions derived from Ni-Ybt complexes, we produced isotopically labeled ^{61}Ni -Ybt (Fig. 3*a*). We performed the cellular uptake assay described in the preceding section (Fig. 2), replacing the exogenous Ni-Ybt with ^{61}Ni -Ybt. We then used inductively coupled plasma MS (ICP-MS) to quantify cell-associated ^{61}Ni -Ybt-derived ^{61}Ni . In this assay, ectopic FyuA expression (UTI89 $\Delta ybtA$ *pfyA*) significantly enhanced cell-associated ^{61}Ni (Fig. 3*b*), consistent with increased periplasmic Ni-Ybt (Fig. 2*b*). When FyuA and YbtPQ are coexpressed (UTI89 $\Delta ybtA$ *pfyA pybtPQ*), however, the ^{61}Ni signal remains cell-associated (Fig. 3*b*). In the context of Ni-Ybt consumption (Fig. 2*b*) and metal-free Ybt production (Fig. 2*c*) in this strain, these data are consistent with cellular nickel retention following YbtPQ-dependent Ni-Ybt dissociation.

Ni-Ybt import nutritionally supports *E. coli* hydrogenase activity

We hypothesized that uropathogens use nickel liberated from Ni-Ybt during YbtPQ-dependent trafficking as a nutrient source for nickel enzymes. We tested this hypothesis by assessing the relationship between Ni-Ybt import and the activity of [NiFe]-hydrogenase isozymes, which have been implicated in UPEC virulence (9). We utilized benzyl viologen to monitor the redox activity of [NiFe]-hydrogenase isozymes (30) in UTI89 grown with different nickel sources. To more specifically assess Ni-Ybt-dependent hydrogenase activity, we created UTI89 mutants in which the canonical *E. coli* nickel import system (NikABCDE) (31) is inactivated (UTI89*nikA::Cml*^R). We then compared [NiFe]-hydrogenase activity between UTI89*nikA::Cml*^R and an isogenic YbtPQ mutant (UTI89*nikA::Cml*^R*pybtPQ::*

Ybt-mediated nickel acquisition

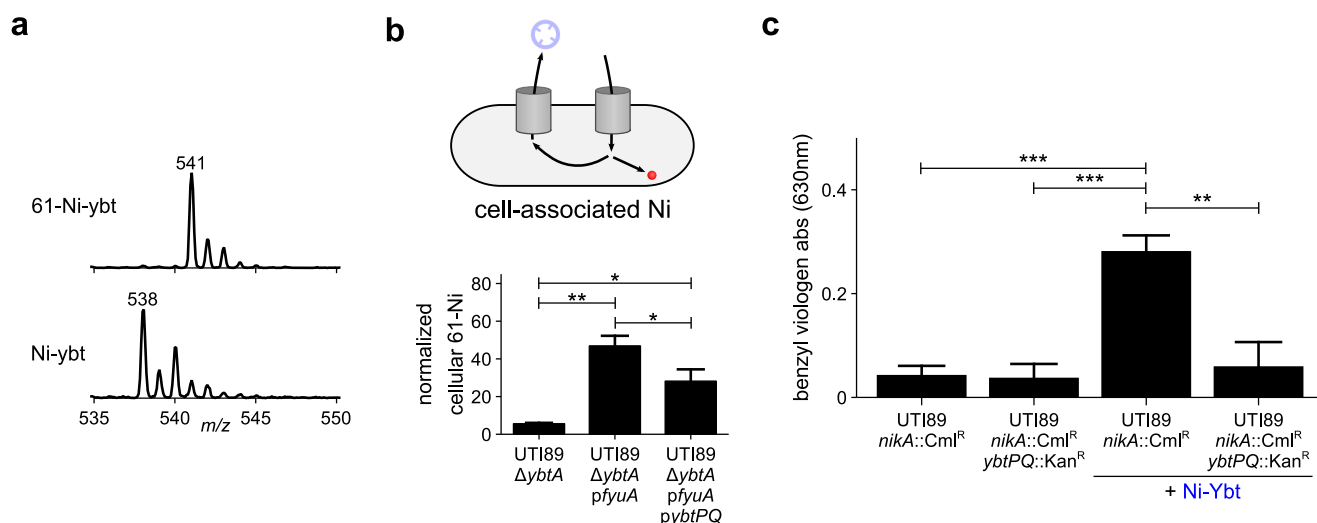


Figure 3. Ybt-derived nickel is retained and supports [NiFe]-hydrogenase activity in uropathogenic *E. coli*. To determine the fate of the nickel ions, the uptake experiment shown in Fig. 2 was repeated with isotopically labeled ⁶¹Ni-Ybt. *a*, the purity of ⁶¹Ni-Ybt was assessed by LC-MS as compared with Ni-Ybt. *b*, the cellular nickel content was measured by ICP-MS. ⁶¹Ni content was normalized to the content of the naturally abundant ⁶⁰Ni isotope. The cartoon indicates which component of the uptake pathway was monitored. *c*, UTI89 $nika::Cml^R$ and UTI89 $nika::Cml^R$ ybtPQ::Kan^R cells were grown in oxygen-limited conditions with or without addition of exogenous Ni-Ybt. The [NiFe]-hydrogenase reduction activity of the cells was observed upon addition of benzyl viologen to the cultures. The [NiFe]-hydrogenase activity was quantified by measuring the increase in absorbance at 630 nm after 10 min. The experiment was performed in triplicate, results are shown as mean \pm S.D. *, $p < 0.05$; **, $p \leq 0.01$; ***, $p \leq 0.001$ based on a *t* test (two-tailed). Unmarked comparisons are nonsignificant.

Kan^R). In the hydrogenase assay growth condition, hydrogenase activity in all *nika*-deficient UTI89 strains depended upon NiCl₂ supplementation (supporting Fig. S1). In the absence of supplemental nickel, *nika*-deficient UTI89 possessed very low hydrogenase activity. Ni-Ybt supplementation (1.2 μ M) significantly ($p < 0.01$) increased hydrogenase activity in UTI89 $nika::Cml^R$ but not YbtPQ-deficient UTI89 $nika::Cml^R$ ybtPQ::Kan^R (Fig. 3c). Together, these findings suggest that uropathogenic *E. coli* can use Ybt-mediated nickel acquisition to nutritionally support [NiFe]-hydrogenase activity.

Ni-Ybt nutritionally supports *Klebsiella* urease activity

Urease is a nickel-dependent enzyme with a long-standing connection to enterobacterial urinary tract virulence (25). Although most *E. coli* isolates lack urease, *Klebsiella*, an often antibiotic-resistant genus in the *Enterobacteriaceae* family, frequently possess urease activity (32). As with *E. coli*, clinical *Klebsiella* isolates often carry the *Yersinia* HPI (33). To determine whether *Klebsiella* can use Ni-Ybt-derived nickel to support urease activity, we identified two urease-positive *Klebsiella pneumoniae* isolates (TOP1856-1 and TOP1993-1) that differ in possession of an active *Yersinia* HPI (Fig. 4a-c). During growth in media conditions associated with high levels of *Klebsiella* urease expression (34), media supplementation with NiCl₂ (1 μ M) increased urease activity of both strains. In contrast, media supplementation with an equimolar quantity of Ni-Ybt (1 μ M) increased urease activity only in TOP1856-1, the isolate with an active *Yersinia* HPI (Fig. 4d). Together, these data show that *Klebsiella* can use the *Yersinia* HPI to nutritionally support the activity of urease, an established urovirulence factor.

Discussion

Although originally appreciated for its siderophore activity, Ybt has recently been found to act as a promiscuous chelator

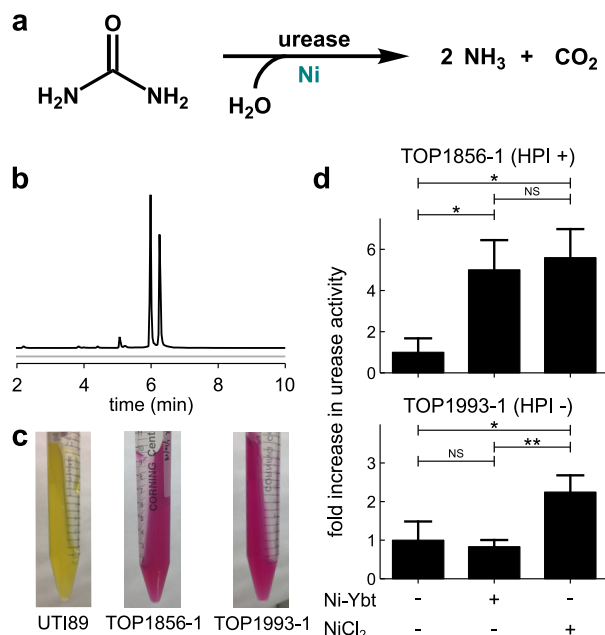


Figure 4. Ni-Ybt import supports urease activity in *Klebsiella pneumoniae*. *a*, the Ni-dependent urease enzyme catalyzes hydrolysis of urea, releasing ammonia and carbon dioxide. *b*, LC-MS analysis of the conditioned media from cultures of the two *K. pneumoniae* isolates, TOP1856-1 (black) and TOP1993-1 (gray). Only TOP1856-1 produces Ybt. Ion chromatograms are presented with identical scaling. *c*, TOP1856-1 and TOP1993-1, as compared with UTI89, are positive for urease activity using Christensen's urea agar test (59). *d*, the *K. pneumoniae* isolates, TOP1856-1 and TOP1993-1, were grown in a minimal media (W4) optimized for high urease expression (34). Addition of NiCl₂ (1 μ M) significantly enhanced urease activity of both strains, whereas addition of purified Ni-Ybt (1 μ M) only enhanced urease activity for the HPI-positive strain TOP1856-1. Urease activity is shown relative to the unsupplemented condition. Data are shown as mean \pm S.D. *, $p \leq 0.05$; **, $p \leq 0.01$ based on a *t* test (two-tailed); NS, nonsignificant.

of biological transition metal ions. Here, we find that uropathogenic *E. coli* use Ybt as a Ni(II) ligand and import the resulting Ni-Ybt complexes to support nutritional demands

for nickel. Both *E. coli* and *Klebsiella* direct Ni–Ybt–derived nickel to different intracellular nickel enzymes. The *Yersinia* high pathogenicity island can thereby function as a second nickel import pathway in uropathogenic enterobacteria. These observations expand our knowledge of the *Yersinia* HPI biometal repertoire and may account for some of its virulence associations.

Uropathogens expressing the Ybt system may be better equipped to obtain nickel during human infections—a benefit which may justify the metabolic cost of Ybt production (35). Infection environments contain a complicated mixture of metal ions and chelators and are characterized by low nickel bioavailability. Nickel content in a host is generally low (~3 nmol per liter (36) and ~40 nmol per liter (13) in serum and urine, respectively), and the ability of host nickel-binding proteins to competitively bind Ni(II) may pose a further challenge to infecting bacteria. One such candidate is the human innate immune protein calprotectin (S100A8/S100A9 heterodimer), which appears at bacterial infection sites and can bind Ni(II) sufficiently to restrict *Staphylococcus aureus* and *K. pneumoniae* urease activity (37). Within the host, nickel appears to exist predominantly in complex with biological ligands (15, 16), suggesting that other, as yet unidentified, nickel-binding innate immune effectors contribute further to physiological nickel restriction. In this context of limited nickel availability, Ybt may provide a competitive advantage over the conserved NikABCDE nickel uptake system. The stable 1:1 Ybt:Ni(II) complexes (18, 38) offer an entropic binding advantage over the 2:1 L-histidine:Ni(II) complexes of the NikABCDE system (17, 39), a feature that would facilitate nickel ion liberation from host-derived complexes. Indeed, a recent comparative binding study indicates that the Ybt Ni(II) binding affinity may be comparable to that of Fe(III) (38), for which an extremely low stability constant of 4×10^{-36} has been reported (40). Which metals ions are bound by Ybt, and whether transport of a particular metal–Ybt species is favored, at an infection site is not yet known. Nonetheless, uptake of Ni– and Fe–Ybt appears to proceed relative to their respective abundances (18). Thus, the Ybt system likely offers a nickel uptake advantage in an extremely context-dependent manner. Future studies are necessary to identify physiological coordination environments which favor bacterial metallophore-based nickel import systems over the canonical Nik system.

Given its ability to mediate nickel import, the observation that Ybt also protects UPEC from nickel toxicity presents an apparent paradox—Ybt mediates both import and detoxification—similar to that observed for Ybt and copper (7, 8). This can be resolved by a model in which bacteria secrete Ybt in excess of local metal levels, creating an extracellular transition metal ion sink from which the secreting cell may import metal–Ybt complexes in a controlled manner. Given the intracellular targets of nickel and copper toxicity (27, 41, 42), the extracellular localization of excess metal–Ybt complexes renders these metals less reactive (passivation) to bacteria; meanwhile, the complexes can be imported and processed as needed to maintain nutritional access to necessary metal ions. This model, recently termed “nutritional passivation,” may thereby explain how the Ybt system confers advantages

to bacteria confronted by both metal scarcity and toxicity (43). Precisely how metal–Ybt complex import is controlled remains unclear. Controlling transport rates may be sufficient to prevent overaccumulation of toxic metal ions by serving as a dam which moderates metal–Ybt delivery. Whether import of different metal–Ybt complexes is differentially regulated is not yet clear. Much remains to be learned about how a single metallophore system accommodates multiple metal ion interactions.

Although the Rcn efflux system (44–46) of *E. coli* protects against *in vitro* nickel toxicity, it is unclear where Rcn- or Ybt-mediated nickel passivation might be useful to uropathogenic enterobacteria. Another nickel efflux pump in *Helicobacter pylori*, CznABC, has been shown to play a role in gastric colonization in a gerbil model (47). It is possible that nickel toxicity is relevant in an environmental niche involved in uropathogenic *E. coli* transmission or pathogenesis and that this favors bacteria carrying the *Yersinia* HPI. Whatever the environment, cytosolic penetration of nickel ions appears to be critical to nickel toxicity (27). Indeed, nickel delivery to enzyme active sites proceeds through cytosolic metallochaperones (48–50). Ybt may augment Rcn-mediated nickel clearance by acting as an extracellular sink that keeps exported nickel ions localized to the extracellular space.

In the present study, we demonstrate that the *Yersinia* HPI–encoded proteins FyuA, YbtP, and YbtQ are necessary for controlled nickel import (as Ni–Ybt) and that this can support nickel enzyme activity. These results identify nickel as the third transition metal (after iron and copper) to exhibit FyuA/YbtPQ-dependent import. By importing nickel ions through designated transporters, the cell is presumably able to maintain control over the rate of nickel delivery. Although TonB/ExbB/ExbD-dependent transport systems such as FyuA are classically associated with iron import, they have also been implicated in nickel uptake by *H. pylori* (51). This Ni–Ybt import pathway is distinct from the putative zinc import activity associated with the *Yersinia* HPI in *Y. pestis* that is thought to proceed via YbtX (52, 53). Where metal–Ybt import and trafficking pathways diverge to direct each ion to its distinctive metalloenzymes or storage proteins remains unclear. It is possible that a single promiscuous reductive dissociation mechanism yields metal-free Ybt from Fe(III), Cu(II), and Ni(II) complexes (8), although the higher Ni(II) reduction potential poses a more formidable energetic barrier. Specific metal chaperones may help traffic reduced ions to their respective destinations during this process, although this remains unclear.

Since Ybt was identified as a nickel-binding metallophore, subsequent studies have identified staphylopin and pseudopaline as metallophores capable of mediating nickel import in *S. aureus* and *Pseudomonas aeruginosa*, respectively (18, 54, 55). For these metallophores, it remains unclear whether nickel binding and import are incidental or if they are part of a valuable nutritional delivery pathway. In the present study, we demonstrate that natively regulated Ni–Ybt import supports [NiFe]-hydrogenase and urease activities, confirming the ability of Ybt to mediate nutritive nickel acquisition. Related approaches may help identify

Ybt-mediated nickel acquisition

Table 1
Strains used in this study

Strain	Relevant properties	References
WT UTI89	A clinical isolate of uropathogenic <i>E. coli</i>	26
UTI89 Δ entB	UTI89 with deletion of EntB, an isochorismate lyase needed for catecholate siderophore production. Strain lacks the ability to produce enterobactin and salmochelin and is used to produce and purify Ybt	3
UTI89 Δ ybtS	UTI89 with deletion of YbtS, a salicylate synthase on the Ybt HPI. Strain is deficient for Ybt production	29
UTI89 Δ ybtA	UTI89 with deletion of the Ybt HPI AraC-type transcriptional regulator YbtA. Strain is deficient for Ybt synthesis and uptake	29
UTI89 Δ ybtA pfyuA	UTI89 Δ ybtA ectopically expressing FyuA off a pTrc99a plasmid	8
UTI89 Δ ybtA pfyuA pybtPQ	UTI89 Δ ybtA ectopically expressing both FyuA (off pTrc99a) and YbtPQ (off a modified pBAD33 plasmid)	8
UTI89nikA::Cml ^R	UTI89 with chloramphenicol resistance insert in place of the periplasmic binding component of the nickel import system, NikA	This study
UTI89nikA::Cml ^R ybtPQ::Kan ^R	The same <i>nikA</i> ::Cml ^R mutation was also made in strain UTI89ybtPQ::Kan ^R (6) which has a kanamycin resistance insert in place of the putative Ybt inner membrane heterodimer, YbtPQ	This study
TOP1856-1	Ybt-producing <i>K. pneumoniae</i> isolate	62
TOP1993-1	Ybt-null <i>K. pneumoniae</i> isolate	62

nickel import systems in microbes beyond uropathogenic *Enterobacteriaceae*.

Experimental procedures

Bacterial strains, plasmids, and culture conditions

Bacterial strains used in this study are listed in Table 1. Starter cultures were grown on LB agar, or in LB medium with antibiotics as appropriate. Ampicillin (100 μ g/ml; Gold Biotechnology), chloramphenicol (34 μ g/ml; Gold Biotechnology), and/or kanamycin (100 μ g/ml; Gold Biotechnology) were used for plasmid selection and knockout screens. Arabinose (0.2%) was used for induction of the pBAD33-based plasmid. In-frame *nikA* deletions were made with the red recombinase method reported previously, using pKD3 as a template and the primers listed in supporting Table S1 (56, 57). The deletions were confirmed with PCR using flanking primers (supporting Table S1).

LC-MS

LC-MS analyses were conducted with a ultra fast LC-equipped AB Sciex 4000 QTRAP with a Turbo V ESI ion source run in positive ion mode (Shimadzu, Kyoto, Japan). The samples were injected onto a phenylhexyl column (100 \times 2.1 mm, 2.7- μ m particle) (Ascentis Express, Supelco, Bellefonte, PA) with a flow rate of 0.4 ml/min and gradient elution over 6 min, from 80% solvent A (0.1% (v/v) formic acid) to 35% solvent A over the first 4 min and then from 35% solvent A to 98% solvent B (90% (v/v) acetonitrile in 0.1% formic acid (v/v)) over the last 2 min. The ion spray voltage was set to 5 kV. The heater temperature was 500 $^{\circ}$ C. The declustering potential, nebulizer gas (G1), and auxiliary gas (G2) were set at 110, 40, and 35 V, respectively.

Detection of yersiniabactin in conditioned media

Overnight cultures of WT UTI89 and UTI89 Δ ybtS were washed once in PBS (Sigma), resuspended in PBS to an A_{600} of 1.0, inoculated 1:100 in M9 glucose minimal media (128 g/liter Na₂HPO₄·7H₂O, 30 g/liter KH₂PO₄, pH 7.4, 5 g/liter NaCl, 1 mg/ml NH₄Cl, 2 mM MgSO₄, 0.1 mM CaCl₂, 0.2% glucose, 10 μ g/ml niacin) and grown for 19 h. No metal ions were added unless specified. The conditioned media were clarified and applied to conditioned C18 silica columns (50 mg, United Chemical Technologies, Bristol, PA), washed with 10% methanol, and eluted in 80% methanol. Eluents were then

analyzed by LC-constant neutral loss-MS (LC-CNL-MS) using the LC-MS settings described above. The constant neutral loss scan was set to detect all parent ions with a common neutral fragment loss of 187 m/z units upon collision-induced dissociation with a collision energy of 30 V. This method has been shown to detect all complexed forms of Ybt described to date (7, 18).

Growth curves

Overnight cultures of WT UTI89 and UTI89 Δ ybtS were washed once in PBS, resuspended in PBS to an A_{600} of 1.0, and inoculated 1:100 in M9 glucose minimal media in a 96-well plate (Corning). The plate was shaken at 37 $^{\circ}$ C and the A_{600} was monitored every hour using a TECAN Spark plate reader. Experiments were repeated at least three times from independent bacterial cultures.

Yersiniabactin preparation

UTI89 Δ entB was grown overnight for 20 h in 500 ml YESCA or M63 minimal media (0.5 M potassium phosphate, pH 7.4, 10 g/liter (NH₄)₂SO₄, 2 mM MgSO₄, 0.1 mM CaCl₂, 0.2% glycerol, 10 μ g/ml niacin) supplemented with 20 μ M salicylate, and 20 μ M dipyriddy. The clarified supernatant was applied to a methanol-conditioned C18 silica column (Sigma), washed, and eluted with 80% methanol. Eluates were concentrated through lyophilization. The dried sample, containing crude, metal-free Ybt, was resuspended in 1 ml water. For pure metal-free Ybt, the crude sample was purified through HPLC using a C18 silica column (Whatman). Fractions containing pure Ybt were collected, lyophilized, and resuspended in water. Concentrations of metal-free Ybt were determined using the Chrome Azurol S assay (58).

Ni-Ybt was prepared by adding NiCl₂ to the crude, metal-free Ybt fraction. Following incubation at room temperature this mixture was applied to a second methanol-conditioned C18 column, washed, and eluted in 80% methanol. The eluent was then lyophilized, resuspended in water, and purified through HPLC as above.

For ⁶¹Ni-Ybt preparation, the crude, metal-free Ybt was first purified through HPLC as described above. A ⁶¹Ni solution was prepared by neutralizing the commercially available Nickel-61 ICP-MS standard in 5% HNO₃ (Inorganic Ventures) with NaHCO₃. This neutralized ⁶¹Ni solution was added to the HPLC-purified Ybt to 147 μ M. The mixture was applied to a

methanol-conditioned C18 column (200 mg, Waters), eluted in 80% methanol, lyophilized, and resuspended in water. The purity of ^{61}Ni -Ybt was assessed by LC-MS/MS using multiple reaction monitoring to detect the precursor/product ion pair characteristic of ^{61}Ni -Ybt (541:354). Final Ni-Ybt concentrations were calculated using the published extinction coefficients (18).

[$^{13}\text{C}_{21}$] Ga-Ybt internal standard was prepared by growing UTI89 Δ *entB* in M63 with [$^{13}\text{C}_3$] glycerol. The supernatant was purified over a methanol-conditioned C18 column (200 mg, Waters).

Cellular uptake of Ni-Ybt

Starter cultures of UTI89 Δ *ybtA*, UTI89 Δ *ybtA* *pfyuA*, and UTI89 Δ *ybtA* *pfyuA* *pybtPQ*, were grown in M63 for 20 h with the appropriate antibiotics and 0.2% arabinose. Cultures were spun down and resuspended in fresh M63 to an A_{600} of 1.5. 2.5 ml of each culture was then plated in 12-well plates (Corning) containing 0.2% arabinose and HPLC-purified Ni-Ybt (0.2 μM). Cultures were incubated for 2 h at 37 °C with shaking. The cells and supernatant from 1 ml cultures were separated by spinning at 20,817 rcf for 10 min at 4 °C.

Cells were washed two times with ice-cold PBS and lysed by resuspension in ice-cold ethanol. Ethanol lysates were rotated at 4 °C for 10 min, clarified at 20,817 rcf for 10 min at 4 °C and dried down *in vacuo*. Dried lysates were resuspended in 1 ml water. Supernatants and resuspended lysates were processed by adding purified [$^{13}\text{C}_{21}$] Ga-Ybt internal standard (20 μl) prior to loading onto conditioned C18 silica columns (50 mg, United Chemical Technologies, Bristol, PA), washing with 10% methanol, and eluting in 80% methanol. The eluents were assessed for Ni-Ybt and metal-free Ybt by LC-MS/MS using the conditions described above. Multiple reaction monitoring was used to specifically detect the precursor/product ion pairs characteristic of [$^{13}\text{C}_{21}$] Ga-Ybt (569:374), Ni-Ybt (538:351), and metal-free Ybt (482:295) using a collision energy of 35 V. Ni-Ybt and metal-free Ybt levels were quantified by normalizing the peak area to that of the [$^{13}\text{C}_{21}$] Ga-Ybt peak area. Standard curves of purified Ni-Ybt and metal-free Ybt with [$^{13}\text{C}_{21}$] Ga-Ybt internal standard were run in the same manner to convert peak area ratios to nanomoles. Experiments were repeated at least three times from independent bacterial cultures.

Cellular uptake of ^{61}Ni -Ybt

Strains were grown and processed as for the cellular uptake assay described above, except that 23 ml of each culture was incubated with HPLC-purified ^{61}Ni -Ybt (0.2 μM). 20 ml of bacteria was harvested at 3197 rcf for 20 min at 4 °C, washed three times with cold PBS and then subjected to microwave digestion in 70% trace metal grade HNO_3 prior to quantification of total cellular nickel content by inductively coupled plasma MS (ICP-MS, PerkinElmer). The abundance of ^{61}Ni was normalized to the amount of the naturally abundant ^{60}Ni isotope. Although ^{58}Ni is more abundant than ^{60}Ni , its detection by ICP-MS is subject to interference from an iron isotope of the same mass. Because iron is often present in excess over nickel, it was there-

fore preferable to monitor ^{60}Ni . Experiments were repeated three times.

[NiFe]-hydrogenase assay

The activity of [NiFe]-hydrogenase was assessed using an adapted benzyl viologen reduction assay.⁴ Briefly, overnight cultures of UTI89*nikA*::Cml^R and UTI89*nikA*::Cml^R*ybtPQ*::Kan^R were inoculated 1:800 in a nickel-limited, rich TYET medium (10 g/liter tryptone, 5 g/liter yeast extract, 50 mM Tris buffer, pH 7.5, 0.4% glucose, 30 mM HCOONa, 1 μM Na₂SeO₃, 1 μM Na₂MoO₄) containing HPLC-purified Ni-Ybt (1 μM) or NiCl₂ (1 mM), as desired, and grown in a 96-well plate at 37 °C for 6 h without shaking. Developing solution (10 mg/ml benzyl viologen, 250 mM HCOONa, 20 mM Tris buffer, pH 7.5) was added to each well and benzyl viologen reduction was measured spectrophotometrically (λ_{max} = 533 nm). Experiments were repeated at least three times from independent bacterial cultures.

Christensen's urea agar test

Urease activity was assessed by plating 10 μl of an overnight LB culture on a urease agar slant (20 g/liter agar, autoclaved, supplemented with 1 g/liter peptone, 1 g/liter dextrose, 5 g/liter NaCl, 2 g/liter potassium phosphate, 20 g/liter urea, 12 mg/liter phenol red before cooling). A color change from yellow to pink was indicative of urease activity (59).

Urease assay

A phenol hypochlorite assay was used to assess the urease activity of lysates (37, 60). Briefly, LB starter cultures were inoculated 1:100 into W4 minimal N media (34, 61) (93 mM potassium phosphate, pH 7.4, 0.4% glucose, 1.74 g/liter glutamic acid, 0.83 mM MgSO₄, 10 $\mu\text{g}/\text{ml}$ niacin) and grown for 20 h. 1 ml of cells was harvested by spinning at 20,817 rcf, 4 °C for 10 min. The conditioned supernatant was saved and processed as described above for analysis of Ybt content. The cells were washed two times with 50 mM HEPES, pH 7.5, resuspended in 0.5 ml HEPES buffer containing lysozyme (1 mg/ml), and incubated at 37 °C for 30 min followed by three freeze/thaw cycles to lyse. 245 μl of each clarified lysate was mixed with 5 μl urea to a final concentration of 20 mM and incubated at 37 °C. Ammonia production was assessed by addition of 375 μl phenol plus nitroprusside (Sigma) followed by addition of 375 μl alkaline hypochlorite (Sigma) and mixing. Samples were incubated at room temperature for 30 min prior to measurement of absorbance at 625 nm. Samples were corrected for background by subtracting the absorbance of lysate handled identically but without addition of urea. Absorbance was converted to moles of ammonia by assessing a series of NH₄Cl standards in the same manner. Experiments were repeated three times from independent bacterial cultures.

Author contributions—A. E. R., E.-I. K., and J. P. H. conceptualization; A. E. R., J. E. L., and E.-I. K. investigation; A. E. R. visualization; A. E. R., E.-I. K., and J. P. H. methodology; A. E. R., J. E. L., and J. P. H. writing-original draft; A. E. R., E.-I. K., and J. P. H. writing-review and editing; J. P. H. supervision; J. P. H. funding acquisition.

⁴ M. J. Lacasse, J. P. Côté, E. D. Brown, and D. B. Zamble, manuscript in preparation.

Acknowledgments—ICP-MS was performed by the Nano Research Facility at Washington University in St. Louis. We thank D. Zamble and M. Lacasse for assistance with the [NiFe]-hydrogenase assay and the laboratory of S. Hultgren for the *Klebsiella* isolates. We also thank W. McCoy IV for helpful discussions.

References

- Gupta, K., Hooton, T. M., Naber, K. G., Wullt, B., Colgan, R., Miller, L. G., Moran, G. J., Nicolle, L. E., Raz, R., Schaeffer, A. J., and Soper, D. E. (2011) International clinical practice guidelines for the treatment of acute uncomplicated cystitis and pyelonephritis in women: A 2010 update by the Infectious Diseases Society of America and the European Society for Microbiology and Infectious Diseases. *Clin. Infect. Dis.* **52**, e103–e120 [CrossRef Medline](#)
- Ohlemacher, S. I., Giblin, D. E., d'Avignon, D. A., Stapleton, A. E., Trautner, B. W., and Henderson, J. P. (2017) Enterobacteria secrete an inhibitor of *Pseudomonas* virulence during clinical bacteriuria. *J. Clin. Invest.* **127**, 4018–4030 [CrossRef Medline](#)
- Henderson, J. P., Crowley, J. R., Pinkner, J. S., Walker, J. N., Tsukayama, P., Stamm, W. E., Hooton, T. M., and Hultgren, S. J. (2009) Quantitative metabolomics reveals an epigenetic blueprint for iron acquisition in uropathogenic *Escherichia coli*. *PLoS Pathog.* **5**, e1000305 [CrossRef Medline](#)
- Hagan, E. C., Lloyd, A. L., Rasko, D. A., Faerber, G. J., and Mobley, H. L. T. (2010) *Escherichia coli* global gene expression in urine from women with urinary tract infection. *PLoS Pathog.* **6**, e1001187 [CrossRef Medline](#)
- Brumbaugh, A. R., Smith, S. N., Subashchandrabose, S., Himpf, S. D., Hazen, T. H., Rasko, D. A., and Mobley, H. L. T. (2015) Blocking yersiniabactin import attenuates extraintestinal pathogenic *Escherichia coli* in cystitis and pyelonephritis and represents a novel target to prevent urinary tract infection. *Infect. Immun.* **83**, 1443–1450 [CrossRef Medline](#)
- Koh, E.-I., Hung, C. S., and Henderson, J. P. (2016) The yersiniabactin-associated ATP binding cassette proteins YbtP and YbtQ enhance *Escherichia coli* fitness during high-titer cystitis. *Infect. Immun.* **84**, 1312–1319 [CrossRef Medline](#)
- Chaturvedi, K. S., Hung, C. S., Crowley, J. R., Stapleton, A. E., and Henderson, J. P. (2012) The siderophore yersiniabactin binds copper to protect pathogens during infection. *Nat. Chem. Biol.* **8**, 731–736 [CrossRef Medline](#)
- Koh, E.-I., Robinson, A. E., Bandara, N., Rogers, B. E., and Henderson, J. P. (2017) Copper import in *Escherichia coli* by the yersiniabactin metallophore system. *Nat. Chem. Biol.* **13**, 1016–1021 [CrossRef Medline](#)
- Subashchandrabose, S., Hazen, T. H., Brumbaugh, A. R., Himpf, S. D., Smith, S. N., Ernst, R. D., Rasko, D. A., and Mobley, H. L. T. (2014) Host-specific induction of *Escherichia coli* fitness genes during human urinary tract infection. *Proc. Natl. Acad. Sci. U.S.A.* **111**, 18327–18332 [CrossRef Medline](#)
- Wang, S. C., Li, Y., Ho, M., Bernal, M. E., Sydor, A. M., Kagzi, W. R., and Zamble, D. B. (2010) The response of *Escherichia coli* NikR to nickel: A second nickel-binding site. *Biochemistry* **49**, 6635–6645 [CrossRef Medline](#)
- Chivers, P. T., and Sauer, R. T. (2000) Regulation of high affinity nickel uptake in bacteria: Ni²⁺-dependent interaction of NikR with wild-type and mutant operator sites. *J. Biol. Chem.* **275**, 19735–19741 [CrossRef Medline](#)
- Leitch, S., Bradley, M. J., Rowe, J. L., Chivers, P. T., and Maroney, M. J. (2007) Nickel-specific response in the transcriptional regulator, *Escherichia coli* NikR. *J. Am. Chem. Soc.* **129**, 5085–5095 [CrossRef Medline](#)
- Sieniawska, C. E., Jung, L. C., Olufadi, R., and Walker, V. (2012) Twenty-four-hour urinary trace element excretion: Reference intervals and interpretive issues. *Ann. Clin. Biochem.* **49**, 341–351 [CrossRef Medline](#)
- Shields-Cutler, R. R., Crowley, J. R., Hung, C. S., Stapleton, A. E., Aldrich, C. C., Marschall, J., and Henderson, J. P. (2015) Human urinary composition controls antibacterial activity of siderocalin. *J. Biol. Chem.* **290**, 15949–15960 [CrossRef Medline](#)
- Van Soestbergen, M., and Sunderman, F. W., Jr. (1972) ⁶³Ni complexes in rabbit serum and urine after injection of ⁶³NiCl₂. *Clin. Chim. Acta* **18**, 1478–1484 [Medline](#)
- Oskarsson, A., and Tjälve, H. (1979) Binding of ⁶³Ni by cellular constituents in some tissues of mice after the administration of ⁶³NiCl₂ and ⁶³Ni(CO)₄. *Acta Pharmacol. Toxicol.* **45**, 306–314 [Medline](#)
- Chivers, P. T., Benanti, E. L., Heil-Chapdelaine, V., Iwig, J. S., and Rowe, J. L. (2012) Identification of Ni-(L-His)₂ as a substrate for NikABCDE-dependent nickel uptake in *Escherichia coli*. *Metallomics* **4**, 1043–1050 [CrossRef Medline](#)
- Koh, E.-I., Hung, C. S., Parker, K. S., Crowley, J. R., Giblin, D. E., and Henderson, J. P. (2015) Metal selectivity by the virulence-associated yersiniabactin metallophore system. *Metallomics* **7**, 1011–1022 [CrossRef Medline](#)
- Fetherston, J. D., Bearden, S. W., and Perry, R. D. (1996) YbtA, an AraC-type regulator of the *Yersinia pestis* pesticin/yersiniabactin receptor. *Mol. Microbiol.* **22**, 315–325 [CrossRef Medline](#)
- Lukacik, P., Barnard, T. J., Keller, P. W., Chaturvedi, K. S., Seddiki, N., Fairman, J. W., Noinaj, N., Kirby, T. L., Henderson, J. P., Steven, A. C., Hinnebusch, B. J., and Buchanan, S. K. (2012) Structural engineering of a phage lysin that targets Gram-negative pathogens. *Proc. Natl. Acad. Sci.* **109**, 9857–9862 [CrossRef Medline](#)
- Fetherston, J. D., Bertolino, V. J., and Perry, R. D. (1999) YbtP and YbtQ: Two ABC transporters required for iron uptake in *Yersinia pestis*. *Mol. Microbiol.* **32**, 289–299 [CrossRef Medline](#)
- Cvetkovic, A., Menon, A. L., Thorgersen, M. P., Scott, J. W., Poole, F. L., 2nd, Jenney, F. E., Lancaster, W. A., Praissman, J. L., Shanmukh, S., Vaccaro, B. J., Trauger, S. A., Kalisiak, E., Apon, J. V., Siuzdak, G., Yannone, S. M., Tainer, J. A., and Adams, M. W. W. (2010) Microbial metalloproteomes are largely uncharacterized. *Nature* **466**, 779–782 [CrossRef Medline](#)
- Li, Y., and Zamble, D. B. (2009) Nickel homeostasis and nickel regulation: An overview. *Chem. Rev.* **109**, 4617–4643 [CrossRef Medline](#)
- McDowall, J. S., Murphy, B. J., Haumann, M., Palmer, T., Armstrong, F. A., and Sargent, F. (2014) Bacterial formate hydrogenlyase complex. *Proc. Natl. Acad. Sci.* **111**, E3948–E3956 [CrossRef Medline](#)
- Mobley, H. L., Island, M. D., and Hausinger, R. P. (1995) Molecular biology of microbial ureases. *Microbiol. Rev.* **59**, 451–480 [Medline](#)
- Chen, S. L., Hung, C.-S., Xu, J., Reigstad, C. S., Magrini, V., Sabo, A., Blasiar, D., Bieri, T., Meyer, R. R., Ozersky, P., Armstrong, J. R., Fulton, R. S., Latreille, J. P., Spieth, J., Hooton, T. M., Mardis, E. R., Hultgren, S. J., and Gordon, J. I. (2006) Identification of genes subject to positive selection in uropathogenic strains of *Escherichia coli*: A comparative genomics approach. *Proc. Natl. Acad. Sci. U.S.A.* **103**, 5977–5982 [CrossRef Medline](#)
- Macomber, L., Eley, S. P., and Hausinger, R. P. (2011) Fructose-1,6-bisphosphate aldolase (class II) is the primary site of nickel toxicity in *Escherichia coli*. *Mol. Microbiol.* **82**, 1291–1300 [CrossRef Medline](#)
- Pelludat, C., Brem, D., and Heesemann, J. (2003) Irp9, encoded by the high-pathogenicity island of *Yersinia enterocolitica*, is able to convert chorismate into salicylate, the precursor of the siderophore yersiniabactin. *J. Bacteriol.* **185**, 5648–5653 [CrossRef Medline](#)
- Lv, H., and Henderson, J. P. (2011) *Yersinia* high pathogenicity island genes modify the *Escherichia coli* primary metabolome independently of siderophore production. *J. Proteome Res.* **10**, 5547–5554 [CrossRef Medline](#)
- Gest, H. (1954) Oxidation and evolution of molecular hydrogen by microorganisms. *Bacteriol. Rev.* **18**, 43–73 [Medline](#)
- Wu, L. F., Navarro, C., and Mandrand-Berthelot, M.-A. (1991) The *hydC* region contains a multi-cistronic operon (*nik*) involved in nickel transport in *Escherichia coli*. *Gene* **107**, 37–42 [CrossRef Medline](#)
- Barry, A. L., Bernsohn, K. L., and Thrupp, L. D. (1969) Four-hour urease test for distinguishing between *Klebsiella* and *Enterobacter*. *Appl. Microbiol.* **18**, 156–158 [Medline](#)
- Bachman, M. A., Oyler, J. E., Burns, S. H., Caza, M., Lépine, F., Dozois, C. M., and Weiser, J. N. (2011) *Klebsiella pneumoniae* yersiniabactin promotes respiratory tract infection through evasion of lipocalin 2. *Infect. Immun.* **79**, 3309–3316 [CrossRef Medline](#)

34. Liu, Q., and Bender, R. A. (2007) Complex regulation of urease formation from the two promoters of the *ure* operon of *Klebsiella pneumoniae*. *J. Bacteriol.* **189**, 7593–7599 [CrossRef Medline](#)
35. Lv, H., Hung, C. S., and Henderson, J. P. (2014) Metabolomic analysis of siderophore cheater mutants reveals metabolic costs of expression in uropathogenic *Escherichia coli*. *J. Proteome Res.* **13**, 1397–1404 [CrossRef Medline](#)
36. Hopfer, S. M., Fay, W. P., and Sunderman, F. W., Jr. (1989) Serum nickel concentrations in hemodialysis patients with environmental exposure. *Ann. Clin. Lab. Sci.* **19**, 161–167 [Medline](#)
37. Nakashige, T. G., Zygiel, E. M., Drennan, C. L., and Nolan, E. M. (2017) Nickel sequestration by the host-defense protein human calprotectin. *J. Am. Chem. Soc.* **139**, 8828–8836 [CrossRef Medline](#)
38. Moscatello, N. J., and Pfeifer, B. A. (2017) Yersiniabactin metal binding characterization and removal of nickel from industrial wastewater. *Bio-technol. Prog.* **33**, 1548–1554 [CrossRef Medline](#)
39. Cherrier, M. V., Cavazza, C., Bochet, C., Lemaire, D., and Fontecilla-Camps, J. C. (2008) Structural characterization of a putative endogenous metal chelator in the periplasmic nickel transporter NikA. *Biochemistry* **47**, 9937–9943 [CrossRef Medline](#)
40. Perry, R. D., Balbo, P. B., Jones, H. A., Fetherston, J. D., and DeMoll, E. (1999) Yersiniabactin from *Yersinia pestis*: Biochemical characterization of the siderophore and its role in iron transport and regulation. *Microbiology* **145**, 1181–1190 [CrossRef Medline](#)
41. Macomber, L., and Imlay, J. A. (2009) The iron-sulfur clusters of dehydratases are primary intracellular targets of copper toxicity. *Proc. Natl. Acad. Sci.* **106**, 8344–8349 [CrossRef Medline](#)
42. Macomber, L., Rensing, C., and Imlay, J. A. (2007) Intracellular copper does not catalyze the formation of oxidative DNA damage in *Escherichia coli*. *J. Bacteriol.* **189**, 1616–1626 [CrossRef Medline](#)
43. Robinson, A. E., Heffernan, J. R., and Henderson, J. P. (2018) The iron hand of uropathogenic *Escherichia coli*: The role of transition metal control in virulence. *Future Microbiol.* **13**, 745–756 [CrossRef Medline](#)
44. Rodrigue, A., Effantin, G., and Mandrand-Berthelot, M.-A. (2005) Identification of *rcnA* (*yohM*), a nickel and cobalt resistance gene in *Escherichia coli*. *J. Bacteriol.* **187**, 2912–2916 [CrossRef Medline](#)
45. Blériot, C., Effantin, G., Lagarde, F., Mandrand-Berthelot, M. A., and Rodrigue, A. (2011) RcnB is a periplasmic protein essential for maintaining intracellular Ni and Co concentrations in *Escherichia coli*. *J. Bacteriol.* **193**, 3785–3793 [CrossRef Medline](#)
46. Iwig, J. S., Leitch, S., Herbst, R. W., Maroney, M. J., and Chivers, P. T. (2008) Ni(II) and Co(II) Sensing by *Escherichia coli* RcnR. *J. Am. Chem. Soc.* **130**, 7592–7606 [CrossRef Medline](#)
47. Stähler, F. N., Odenbreit, S., Haas, R., Wilrich, J., Van Vliet, A. H. M., Kusters, J. G., Kist, M., and Bereswill, S. (2006) The novel *Helicobacter pylori* CznABC metal efflux pump is required for cadmium, zinc, and nickel resistance, urease modulation, and gastric colonization. *Infect. Immun.* **74**, 3845–3852 [CrossRef Medline](#)
48. Zeer-Wanklyn, C. J., and Zamble, D. B. (2017) Microbial nickel: Cellular uptake and delivery to enzyme centers. *Curr. Opin. Chem. Biol.* **37**, 80–88 [CrossRef Medline](#)
49. Lacasse, M. J., Douglas, C. D., and Zamble, D. B. (2016) Mechanism of selective nickel transfer from HypB to HypA, *Escherichia coli* [NiFe]-hydrogenase accessory proteins. *Biochemistry* **55**, 6821–6831 [CrossRef Medline](#)
50. Higgins, K. A., Carr, C. E., and Maroney, M. J. (2012) Specific metal recognition in nickel trafficking. *Biochemistry* **51**, 7816–7832 [CrossRef Medline](#)
51. Schauer, K., Gouget, B., Carrière, M., Labigne, A., and de Reuse, H. (2007) Novel nickel transport mechanism across the bacterial outer membrane energized by the TonB/ExbB/ExbD machinery. *Mol. Microbiol.* **63**, 1054–1068 [CrossRef Medline](#)
52. Bobrov, A. G., Kirillina, O., Fetherston, J. D., Miller, M. C., Burlison, J. A., and Perry, R. D. (2014) The *Yersinia pestis* siderophore, yersiniabactin, and the ZnuABC system both contribute to zinc acquisition and the development of lethal septicemic plague in mice. *Mol. Microbiol.* **93**, 759–775 [CrossRef Medline](#)
53. Bobrov, A. G., Kirillina, O., Fosso, M. Y., Fetherston, J. D., Miller, M. C., VanCleave, T. T., Burlison, J. A., Arnold, W. K., Lawrenz, M. B., Garneau-Tsodikova, S., and Perry, R. D. (2017) Zinc transporters YbtX and ZnuABC are required for the virulence of *Yersinia pestis* in bubonic and pneumonic plague in mice. *Metallomics* **9**, 757–772 [CrossRef](#)
54. Ghssein, G., Brutesco, C., Ouerdane, L., Wang, S., Hajjar, C., Lobinski, R., Lemaire, D., Richaud, P., Espallat, A., Cava, F., Pignol, D., and Arnoux, P. (2016) Biosynthesis of a broad-spectrum nicotianamine-like metallophore in *Staphylococcus aureus*. *Science* **352**, 1105–1109 [CrossRef Medline](#)
55. Lhospipe, S., Gomez, N. O., Ouerdane, L., Brutesco, C., Ghssein, G., Hajjar, C., Liratni, A., Wang, S., Richaud, P., Bleves, S., Ball, G., Borezée-Durant, E., Lobinski, R., Pignol, D., Arnoux, P., and Voulhoux, R. (2017) *Pseudomonas aeruginosa* zinc uptake in chelating environment is primarily mediated by the metallophore pseudopaline. *Sci. Rep.* **7**, 17132 [CrossRef Medline](#)
56. Datsenko, K. A., and Wanner, B. L. (2000) One-step inactivation of chromosomal genes in *Escherichia coli* K-12 using PCR products. *Proc. Natl. Acad. Sci.* **97**, 6640–6645 [CrossRef Medline](#)
57. Murphy, K. C., and Campellone, K. G. (2003) Lambda Red-mediated recombinogenic engineering of enterohemorrhagic and enteropathogenic *E. coli*. *BMC Mol. Biol.* **4**, 11 [CrossRef Medline](#)
58. Schwyn, B., and Neilands, J. B. (1987) Universal chemical assay for the detection and determination of siderophores. *Anal. Biochem.* **160**, 47–56 [CrossRef Medline](#)
59. Christensen, W. B. (1946) Urea decomposition as a means of differentiating *Proteus* and *Paracolon* cultures from each other and from *Salmonella* and *Shigella* types. *J. Bacteriol.* **52**, 461–466 [Medline](#)
60. Weatherburn, M. W. (1967) Phenol-hypochlorite reaction for determination of ammonia. *Anal. Chem.* **39**, 971–974 [CrossRef](#)
61. Bender, R. A., Janssen, K. A., Resnick, A. D., Blumenberg, M., Foor, F., and Magasanik, B. (1977) Biochemical parameters of glutamine synthetase from *Klebsiella aerogenes*. *J. Bacteriol.* **129**, 1001–1009 [Medline](#)
62. Czaja, C. A., Stamm, W. E., Stapleton, A. E., Roberts, P. L., Hawn, T. R., Scholes, D., Samadpour, M., Hultgren, S. J., and Hooton, T. M. (2009) Prospective cohort study of microbial and inflammatory events immediately preceding *Escherichia coli* recurrent urinary tract infection in women. *J. Infect. Dis.* **200**, 528–536 [CrossRef Medline](#)

Uropathogenic enterobacteria use the yersiniabactin metallophore system to acquire nickel

Anne E. Robinson, Jessica E. Lowe, Eun-Ik Koh and Jeffrey P. Henderson

J. Biol. Chem. 2018, 293:14953-14961.

doi: 10.1074/jbc.RA118.004483 originally published online August 14, 2018

Access the most updated version of this article at doi: [10.1074/jbc.RA118.004483](https://doi.org/10.1074/jbc.RA118.004483)

Alerts:

- [When this article is cited](#)
- [When a correction for this article is posted](#)

[Click here](#) to choose from all of JBC's e-mail alerts

This article cites 62 references, 25 of which can be accessed free at <http://www.jbc.org/content/293/39/14953.full.html#ref-list-1>